Single-nuclei multiome ATAC and RNA sequencing reveals the molecular basis of thermal plasticity in *Drosophila melanogaster* embryos

Thomas S. O'Leary[1], Emily E. Mikucki[1], Sumaetee Tangwancharoen[1], Joseph R. Boyd[2], Seth Frietze[2], Sara Helms Cahan[1], and Brent L. Lockwood[1]

[1]Department of Biology, University of Vermont, Burlington, VT 05405
[1]Department of Biomedical and Health Sciences, University of Vermont, Burlington, VT 05401

January 7, 2025

Abstract

Embryogenesis is remarkably robust to temperature variability, yet there is limited understanding of the homeostatic mechanisms that offset thermal effects during early development. Here, we measured the thermal acclimation response of upper thermal limits and profiled chromatin state and the transcriptome of *D. melanogaster* embryos (Bownes Stage 11) using single-nuclei multiome ATAC and RNA sequencing. We report that thermal acclimation, while preserving a common set of primordial cell types, rapidly shifted the upper thermal limit. Cool-acclimated embryos showed a homeostatic response characterized by increased chromatin accessibility at transcription factor binding motifs for the transcriptional activator Zelda, along with enhanced activity of gene regulatory networks in the primordial cell types including the foregut and hindgut, mesoderm, and peripheral nervous system. In addition, cool-acclimated embryos had higher expression of genes encoding ribosomal proteins and enzymes involved in oxidative phosphorylation. Despite the hypothesis that differential heat tolerance might be explained by differential expression of molecular chaperones, we did not observe widespread differences in the chromatin accessibility or expression of heat shock genes. Overall, our results suggest that environmental robustness to temperature during embryogenesis necessitates homeostatic gene expression responses that regulate the speed of development, potentially imposing metabolic costs that constrain upper thermal limits.

Introduction

Early embryonic development in *Drosophila* involves the spatially and temporally coordinated activation of zygotic transcription, resulting in precise transcriptional patterning across the embryo [1, 2, 3, 4]. These events culminate in crucial early morphological transitions, such as gastrulation, and the specification of primordial tissues [5, 6, 7, 8, 4]. Such an intricate morphogenetic process would seem to be sensitive to environmental perturbation, and yet embryonic development is characterized by a high level of morphological robustness where embryos are able to maintain consistent developmental outcomes despite environmental and mutational variation [9, 10]. This developmental robustness may arise from a balance between stability and plasticity at the molecular level, where key transcriptional gradients must remain stable across a range of temperatures [11, 12, 13], while other molecular processes need to undergo dynamic adjustments that buffer against environmental changes.

This interplay between stability and plasticity at the molecular level is particularly remarkable because changes in temperature directly impact the rates of biochemical reactions [14] driving changes in the rates of transcription and translation [15, 16]. Indeed, thermal effects on biological rates are so ubiquitous that organisms must adjust via homeostatic mechanisms that actively regulate gene or protein expression [17, 18, 19] to optimize performance across a thermal range [20, 21, 22]. In many organisms, thermal acclimation responses in later development and adulthood are well established [23, 24, 25], suggesting that environmental robustness of embryogenesis may be underpinned by active homeostatic responses. Yet, while beneficial at a specific acclimation temperature, these responses may impose metabolic trade-offs that reduce tolerance to a subsequent acute heat stress.

Embryonic development involves three key complex cellular and molecular events: (i) the hand-off of molecular control from maternal factors to zygotically expressed factors [3, 26, 27], (ii) cellularization, gastrulation, and cell migration [28, 5, 8], and (iii) cell-type specification and tissue differentiation [29, 30]. Despite depending on complex interactions between proteins, DNA, and other macromolecules, all of which may be affected by temperature, these processes remain stable across a range of temperatures [12, 13, 22]. Yet, the underlying mechanisms of environmental robustness have not been fully characterized and the role of thermal phenotypic plasticity during embryogenesis has not been investigated, as the vast majority of studies on embryogenesis have been conducted under static laboratory conditions [29, 31, 32]. This is a critical gap in knowledge because thermal traits influence species survival [33, 34, 35], and the acclimation of upper thermal limits may thus impact the vulnerability of a species to future climate change [36]. Because embryos cannot behaviorally thermoregulate and have a lower thermal limit than later life stages [9, 37], even small shifts in thermal tolerance at this critical stage may contribute significantly to species persistence [38, 37].

Here, we investigated the thermal acclimation potential of heat tolerance of *D. melanogaster* embryos across a 12°C range. Embryonic heat tolerance underwent a rapid acclimation response over a period of several hours, such that heat tolerance tracked acclimation temperature. To elucidate the molecular basis of embryonic thermal acclimation, we utilized a single cell multiomics approach combining single-nuclei ATAC and RNA sequencing of Bownes stage 11 embryos (*i.e.*, the stage of embryogenesis where embryos are nearing the end of multipotency and beginning the process of specification, committing to their final cell fates). This approach allowed direct examination of how rearing temperature impacts cell-type-specific regulation and expression of individual genes, as well as modules of co-expressed genes and entire gene regulatory networks. We hypothesized that the observed plasticity in the upper thermal limit may result from two separate, but non-mutually exclusive, physiological responses. One possibility is that warm-acclimated embryos are more heat tolerant because they actively prepare cellular heat stress defenses as a beneficial acclimation response [39]. For example, heat preparedness may manifest as greater chromatin accessibility and expression of genes that support coping mechanisms, such as heat shock genes [40, 41, 42, 43]. Another possibility is that cool-acclimated embryos are more susceptible to heat stress because they either lack heat preparedness or because cool acclimation involves homeostatic responses that render differentiating cell populations more sensitive to heat. For example, embryos may increase protein synthesis and cellular respiration to compensate for slower kinetics in the cold [44], and this may lead to the accumulation of metabolic byproducts (*e.g.*, reactive oxygen species) that reduce heat tolerance [18, 45, 46, 47]. Our results allow us to evaluate these hypotheses to elucidate the gene-regulatory mechanisms by which *Drosophila* embryos undergo rapid thermal acclimation. Overall, our results show that warm-acclimated embryos exhibited little evidence of enhanced heat preparedness but that cool-acclimated embryos underwent a thermal compensation response, suggesting that the metabolic and cellular trade-offs involved in maintaining homeostasis

at cooler temperatures may be a critical, yet underappreciated, driver of thermal plasticity during embryonic development.

Results

Thermal acclimation rapidly improves embryonic heat tolerance

To establish the phenotypic effect of thermal acclimation—*i.e.*, 9 h at 18°C, 5 h at 25°C, or 3 h at 30°C (see Methods)—we measured hatching success following an acute heat shock of 45 minutes at 38.75°C, a temperature close to the upper thermal limit of embryos at this stage of development (data not shown). Acclimation temperature significantly influenced acute heat tolerance (**Fig. 1**; quasi-binomial logistic regression, $p < 1 \cdot 10^{-5}$), with survival rates improving at higher acclimation temperatures. Survival was approximately 2-fold higher in the 25°C-acclimated embryos, with a 42.6% hatching success, compared to the 18°C-acclimated embryos, which had only 21.0% hatching success. The 30°C -acclimated embryos had the highest survival after acute heat stress at 49.5%.

Single-nuclei multiome sequencing and quality control

Given the high per-sample cost of 10X Multiome sequencing, we focused our analysis on the 18°C and 25°C acclimation conditions, excluding the 30°C acclimated embryos. These two conditions were chosen because they exhibited the largest change in upper thermal limit despite only a 7°C difference in acclimation temperature. To sample embryos for 10X Multiome sequencing, we acclimated embryos to 18°C and 25°C as before and then collected a pool of 50 embryos for each replicate, with two replicates for each acclimation treatment, ultimately aiming to capture approximately 4,000 high-quality nuclei from each single replicate. The sequencing yielded an ATAC-seq library with a total of 262 million high-quality read pairs and an RNA-seq library with a total of 214 million high-quality reads. In total, these reads mapped to 464,722 barcodes with at least one read in both the ATAC-seq and RNA-seq libraries (**Fig. S1 C**). Quality control removed nuclei with low read counts, high mitochondrial or ribosomal content, or suspected multiplets, resulting in a total of 10,390 high-quality nuclei, with 5,298 nuclei from the 18°C acclimated embryos and 5,092 nuclei from the 25°C acclimated embryos (**Fig. S1 A & B**). Per nucleus, there was a median of 983 RNA-seq reads and 5,688 ATAC-seq reads (**Fig. S2 A & B**). Across all nuclei, we detected 11,271 peaks and 9,007 genes, with a median of 2,205.5 peaks and 586 genes per nucleus (**Fig. S2 C & D**).

Primordial cell types remain conserved across acclimation treatments

Following quality control filtering, the remaining 10,390 nuclei were visualized in low-dimensions on a Uniform Manifold Approximation and Projection (UMAP) using data from both the ATAC and RNA sequencing libraries with a weighted k-nearest neighbor approach. Nuclei from the two acclimation treatments showed substantial overlap, indicating conserved developmental trajectories despite temperature differences (**Fig. 2 A**). To identify distinct cell populations within these nuclei, we identified 12 clusters using a shared nearest neighbor of the weighted ATAC and RNA data (**Fig. 2 B**). To annotate these clusters to labels of known cell types, we identified 1,564 cluster-specific marker genes in the expression data (**Fig. 2 D**; **Fig. S5**). Similar to the annotation method used in Calderon *et al.*, 2022 [32], we matched clusters to annotated cell types using a Fisher's enrichment test for annotations of genes present in the Berkeley *Drosophila* Genome Project RNA

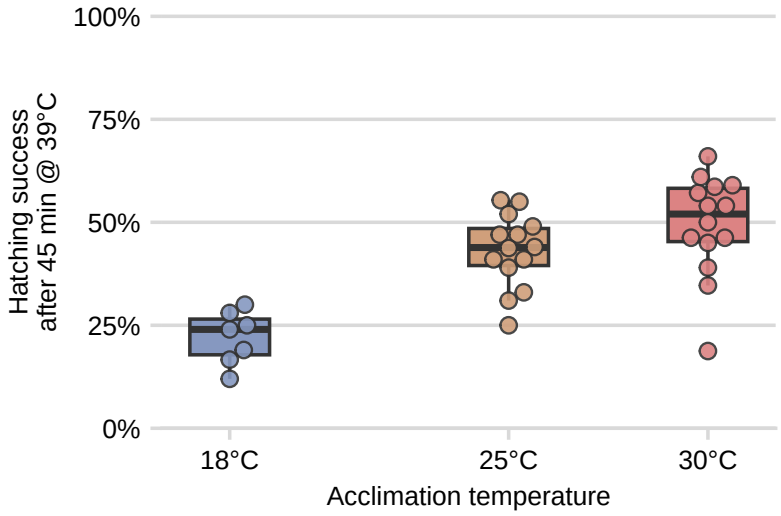

Figure 1: **Thermal acclimation of early embryos led to differential acute heat shock tolerance.** The hatching success of embryos following an acute heat shock of 38.75°C for 45 minutes. Hatching success increased with increasing acclimation temperature (quasi-binomial logistic regression; $p < 1 \cdot 10^{-5}$). Individual dots represent replicate grids of approximately 50 to 100 embryos, total number of eggs per acclimation temperature: 520, 1272, 1145 for 18°C, 25°C, and 30°C respectively.

in situ hybridization [48] and final annotation calls for all Seurat clusters were made manually with the input of these automatic annotations (**Fig. 2 C**).

Concordance between chromatin accessibility and gene expression validates cell-type-specific annotations

To ensure the accuracy of cell-type annotations derived from RNA-seq marker gene data, we assessed the concordance between chromatin accessibility (ATAC-seq) and gene expression profiles. The cell-type-specific data from single-nuclei multiome sequencing revealed strong agreement between RNA-seq-based annotations and ATAC-seq chromatin accessibility patterns. Among the 1,564 cluster-specific marker genes identified, 1,260 (80%) had nearby ATAC-seq peaks that were significantly correlated with gene expression. The top linked peaks (lowest adjusted p-value) exhibited matching cell-type-specific chromatin accessibility patterns, supporting the validity of cell-type assignments (**Fig. 2 E**). Indeed, this strong correlation between the ATAC-seq and RNA-seq data is seen across all identified marker genes and their top linked accessibility peaks, where the cell-type-specific correlations range between 0.55 and 0.66 (**Fig. S4**). To display this concordance between chromatin accessibility and gene expression in more granular detail, we visualized ATAC-seq coverage plot tracks for three top marker genes, *btl*, *Mef2*, and *otp*, for tracheal primordium, mesoderm primordium, and foregut & hindgut primordium, respectively (**Fig. S6**). These coverage plots show cell-type-specific chromatin accessibility that matches increased cell-type-specific expression levels in the RNA-seq data.

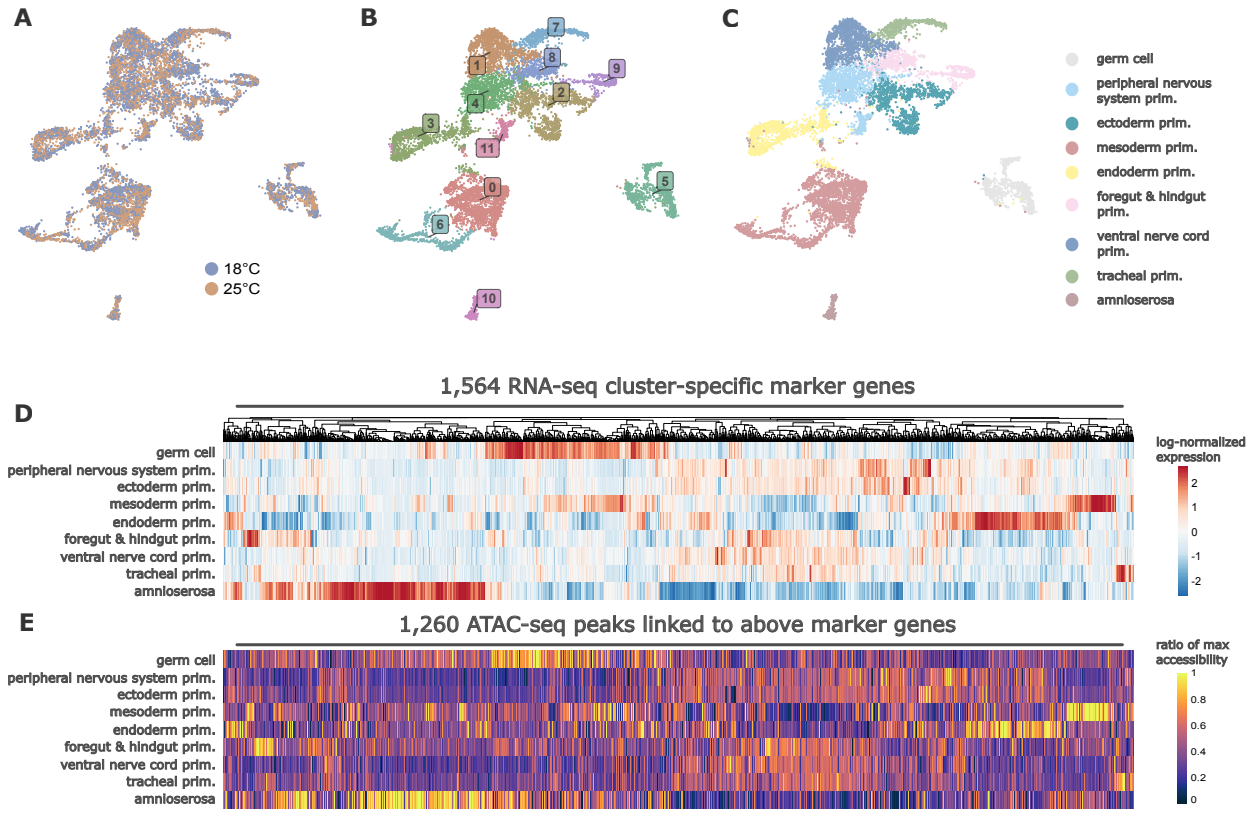

Figure 2: **Nuclei cluster similarly across acclimation states and were annotated to cell-type labels using identified marker genes and there was a strong concordance between ATAC-Seq and RNA-seq data. A.-C.** A UMAP representation of the single nuclei multiome data. Each dot represents an individual nucleus characterized by integrative profiling of gene expression (RNA) and chromatin accessibility (ATAC) condensed into a two-dimensional representation. UMAPs are colored by three different representations, acclimation treatment **(A)**, cluster number **(B)**, and annotated cell types **(C)**. Heatmaps of the RNA-seq cluster specific marker genes **(D)** (color indicates log-normalized expression of aggregated expression values ATAC-seq peaks linked to the maker genes **(E)** (color indicates normalization of minimum and maximum accessibility across cell-types, with low values indicating the least accessible regions and values close to one indicating the maximum observed accessibility).

Target motif analysis reveals differential chromatin accessibility in Zelda and HSF motifs between acclimation temperatures

To conduct the target motif analysis and investigate broad changes in chromatin accessibility across cell types, we combined all the single cell data together for a pseudobulk analysis and performed a test of differentially accessible regions (DARs) on the ATAC-seq data. We found a total of 142 peaks that were differentially accessible between acclimation temperatures, with 84 regions (59 %) with increased accessibility in the cool-acclimated embryos and 58 (41%) more accessible in the warm acclimated embryos (**Fig. S7 A**). To identify motifs overrepresented among the pseudobulk DARs we ran a motif enrichment analysis. Out of the 150 motifs analyzed in the data set, only one target motif was differentially enriched in the pseudobulk DARs, the target motif of the pioneer transcription factor Zelda, which is involved in early zygotic genome activation. Of the 710 Zelda

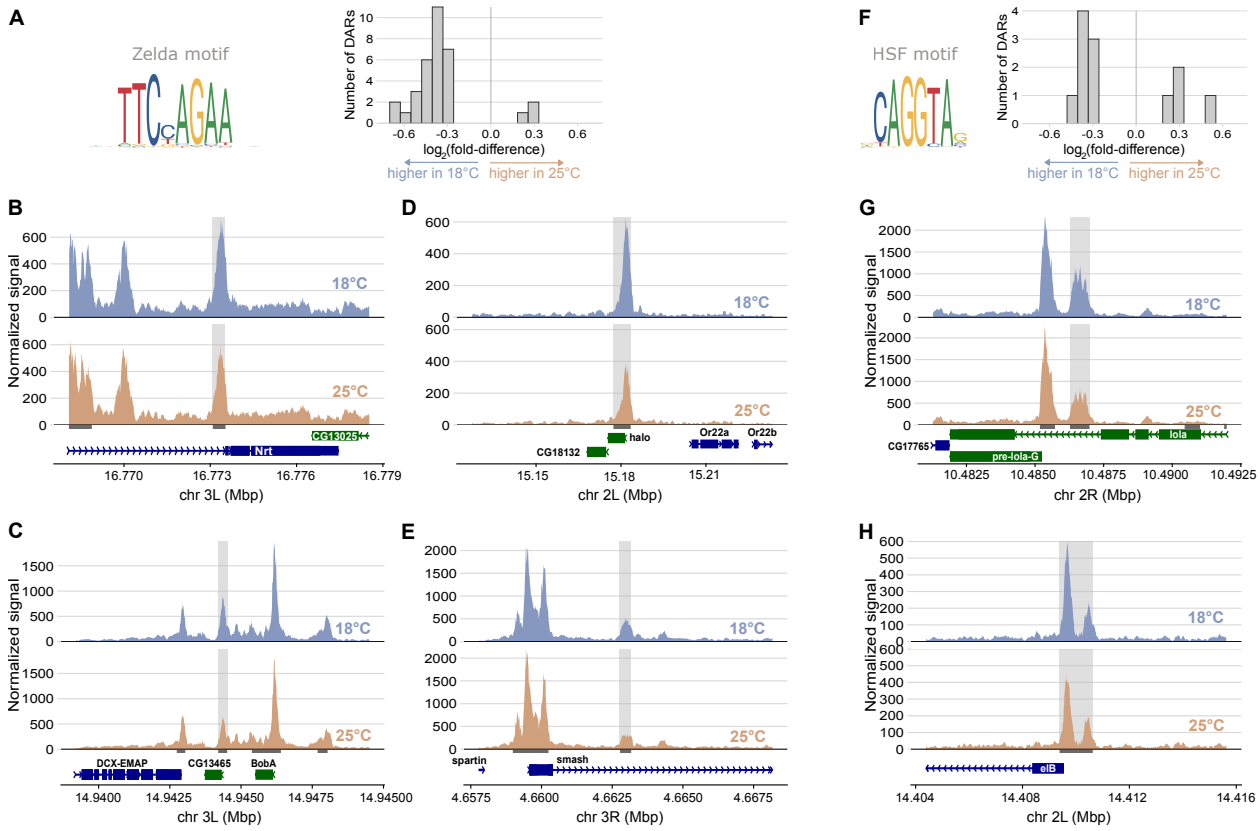

Figure 3: **The majority of pseudobulk DARs with Zelda- or HSF-target motifs show increased accessibility in the 18°C cool-acclimated embryos.** Histograms of $\log_2$ fold-difference between acclimation treatments of the 33 pseudobulk DARs that contain the Zelda-target motif **(A)** and the 12 pseudobulk DARs that contain HSF-target motif **(F)**. Pseudobulk ATAC-seq coverage plots for four representative Zelda-target motif containing DARs **(B-E)** and two representative HSF-target motif containing DARs **(G-H)**. Within each panel containing coverage plots, the top trace colored blue represents the accessibility of the 18°C cool-acclimated embryos, and the bottom trace in orange represents the 25°C warm-acclimated embryos. Grey shading indicates the peak regions with differential accessibility between acclimations.

target motif-containing peaks that were detected in at least 10% of nuclei, 33 were significantly differentially accessible between acclimation treatments, with most of them more accessible in the cool-acclimated embryos (**Fig. 3 A**). GO enrichment of the 33 Zelda-target DARs revealed overrepresentation of developmental processes including axis elongation and cell migration (**Fig. S7 C**). Additionally, to assess the degree to which embryos were prepared for heat stress through changes in the accessibility of heat shock genes prior to heat shock, we looked at the accessibility of peaks that contained HSF target motifs. Of the 518 HSF-target peaks detected in at least 10% of nuclei, there were 12 DARs (**Fig. 3 F**). In contrast to expectations based on the heat-preparedness hypothesis [42], HSF-target motifs were less accessible in the 25°C warm-acclimated embryos (**Fig. 3 F**). Two representative chromatin accessibility tracks of the HSF-target motif containing DARs were visualized (**Fig. 3 G & H**).

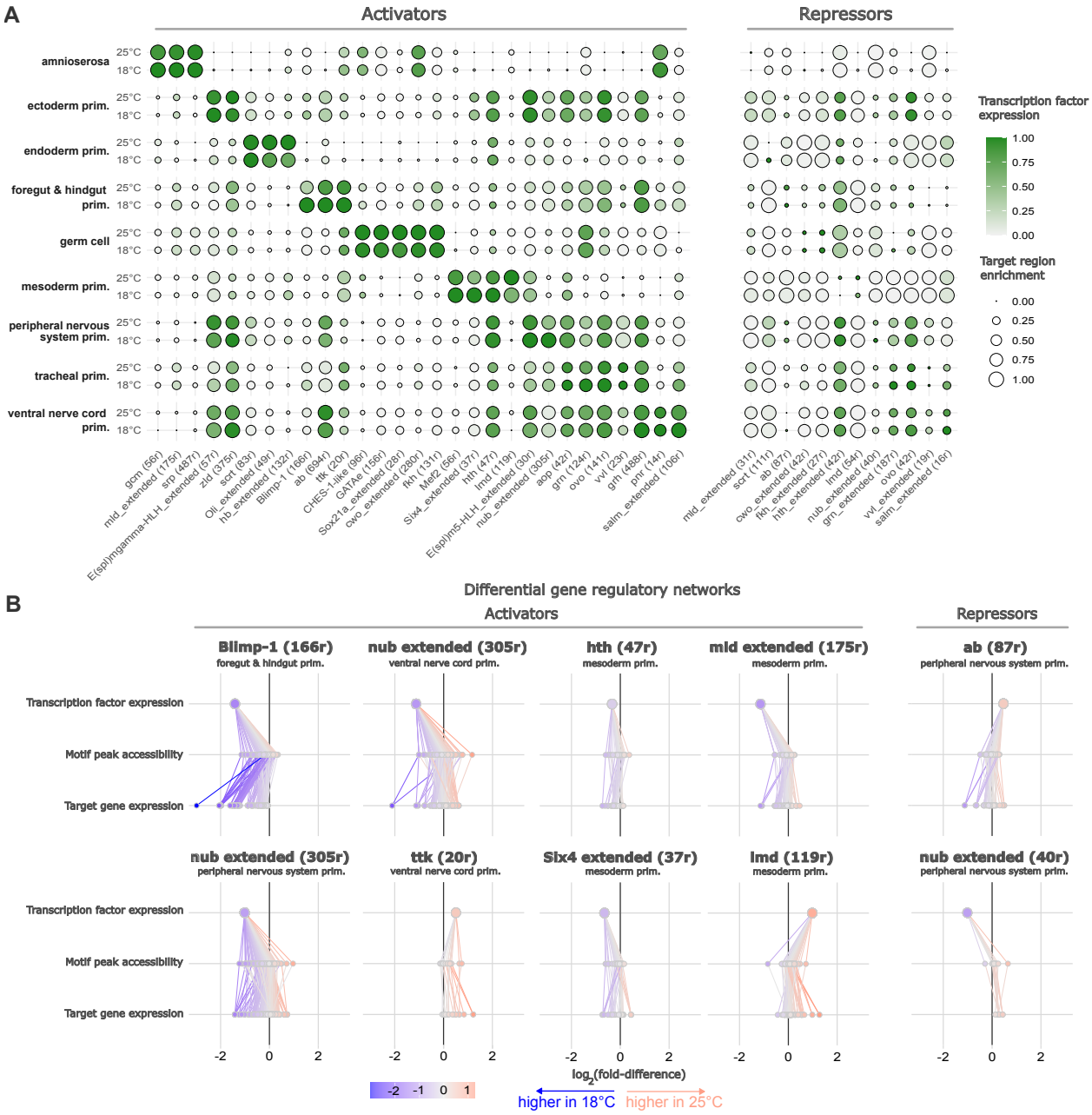

Figure 4: **Ten cell-type-specific GRNs were altered with acclimation temperature, while the rest remained stable despite variation in environmental temperature. A.** SCENIC+ identified eRegulons separated out by cell-type and acclimation, 29 activator eRegulons are on the left panel and 12 repressors are on the right panel. The green color represents normalized transcription factor expression and area of the dot represents target region enrichment with greater size indicating more accessible chromatin. **B.** Ten differential gene regulatory networks (diffGRNs) plotted with $\log_2$ fold-differences for each node in the network. Colored by $\log_2$ fold-difference with red indicating higher expression or accessibility in the 25°C acclimated embryos and blue indicating higher in the 18°C cool-acclimated embryos. diffGRNs labeled as activators are on the left, and repressors are on the right.

Gene regulatory networks reveal differential responses to thermal acclimation

Our analysis revealed that gene regulatory networks were largely unaffected by acclimation temperature, with transcription factor expression and target motif accessibility remaining stable across cell types (**Fig. 4 A**). However, a subset of networks displayed significant alterations in response to acclimation (**Fig. 4 B**). Using the SCENIC+ pipeline [49], we identified 41 enhancer driven GRNs, referred to as eRegulons in SCENIC+ terminology. For simplicity, we will use the term GRN throughout this manuscript to describe these eRegulons, acknowledging that they represent an imputed subset of a broader GRN that may be active. This GRN-based approach is particularly valuable for identifying transcription factors, target motifs, and downstream genes that drive cell-type-specific patterns during embryonic development. Additionally, it allows us to assess whether specific GRNs were altered in response to thermal acclimation. Of the 41 eRegulons with transcription factor expression and cistrome correlation greater than 0.5 ($|\rho| > 0.5$) (**Fig. S8**), 29 eRegulons had transcription factors acting as activators, (*i.e.*, opening the target motif and increasing target gene expression), and 12 eRegulons were found to be repressors (*i.e.*, more transcription factor expression led to decreased target motif accessibility and decreased target gene expression) (**Fig. 4 A**). Some eRegulons represent cell-type-specific transcription factors and marker genes and many of the networks were unchanged with acclimation, but there were several notable differences. A total of 18 transcription factors were differentially expressed within a cell-type between acclimation treatments. Of those 18 transcription factors, 10 gene regulatory networks were differentially regulated (diffGRNs) following thermal acclimation, defined by a shift in accessibility across peaks containing the target motif and a corresponding shift in the expression of the target genes (**Fig. 4 B**). For example, the gene *Blimp-1*, which encodes a transcription factor expressed in the foregut and hindgut primordium at this stage, was significantly upregulated in the cool-acclimated embryos with a $\log_2$ fold-difference of 1.41. The peaks containing target motifs of Blimp-1 were then shifted to positive $\log_2$ fold-differences (one sample t-test; $p = 5.4 \cdot 10^{-13}$). The $\log_2$ fold-differences for the corresponding target genes were also increased in the cool-acclimated embryos (one sample t-test; $p = 1.3 \cdot 10^{-9}$). Overall, 4 out of the 10 diffGRNs were in the mesoderm primordium, and 3 were in the peripheral nervous system primordium, 2 were in the ventral nerve cord primordium, and the remaining one diffGRN was in the foregut and hindgut primordium.

WGCNA reveals acclimation response of co-expressed genes

To gain insight into global gene expression patterns and identify temperature-dependent regulatory changes, we performed high-dimensional weighted gene co-expression network analysis (hdWGCNA) on the single-nuclei RNA-seq data. hdWGCNA identified seven distinct modules of co-expressed genes within the single-nuclei RNA-seq data (**Fig. S9 A**). These modules captured diverse gene expression patterns, with some broadly expressed across cell types and others restricted to specific subsets of annotated cell types (**Fig. S9 B**). The degree of cell type specificity of each module was summarized in a metric we call the cell type specificity index (CTSI) (**Fig. S9 C**), which was calculated as the standard deviation of the mean cell-type-specific module eigengene scores within each module (**Fig. S9 B**). Higher values of CTSI indicate greater cell type specificity. For example, the brown and red modules were broadly represented across nuclei, as exhibited by low CTSI values and the mean cell type module eigengene score being close to zero for all cell types. Other modules were expressed in only a subset of cell types. For example, two modules with relatively high CTSI values included the green module, which was primarily localized to the mesoderm and germ cell primordia, and the yellow module with genes heavily expressed in the amnioserosa but not in other cell types (**Fig. S9 B**).

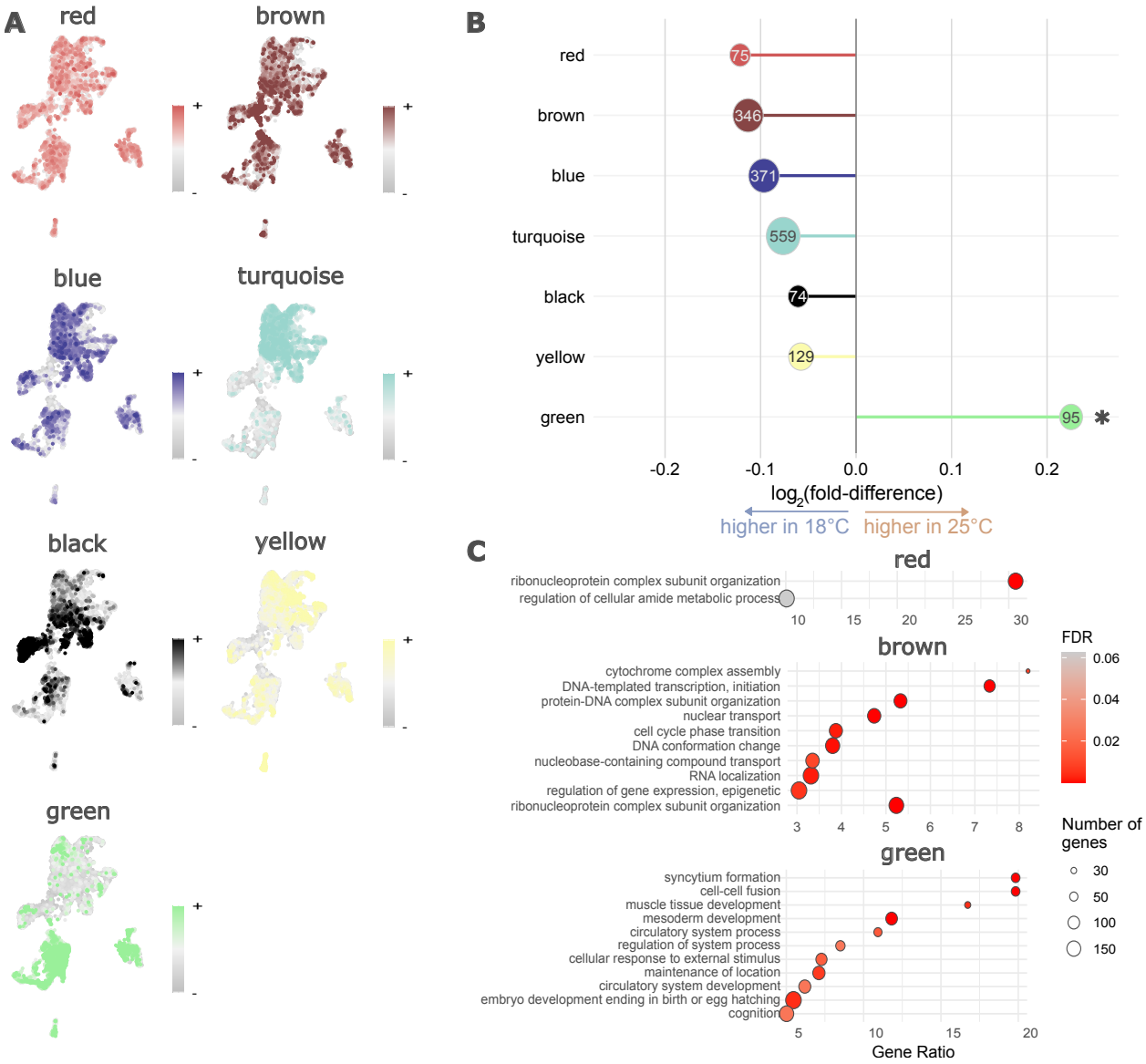

Figure 5: **High-dimensional weighted gene coexpression network analysis (hdWGCNA) on single-nuclei RNA-seq data identifies a few modules of genes that differ in expression following acclimation to different temperatures. A.** UMAPs with each nuclei colored by its module eigengene value. **B.** Module eigengene average $\log_2$ fold-difference in gene expression between acclimation states for each module. Inset number is the total number of genes per module, with the points sized proportional to module size. Asterisk indicates significance of DME test. **C.** The top overrepresented GO terms in the red, brown, and green modules.

Some modules showed differential expression following acclimation, as seen in the module eigengene average expression change between acclimation states (**Fig. 5 B**). Notably, the green module displayed significantly higher expression in 25°C warm-acclimated embryos compared to 18°C cool-acclimated embryos (DME test; $p < 0.05$), highlighting its potential role in temperature-specific transcriptional responses. The green module was enriched for developmental processes, such as mesoderm development, muscle tissue development, and embryonic organ development (**Fig. 5 C**,

Fig. S10 G), reflecting expression in specific cell lineages like the mesoderm and germ cells.

All other modules showed trends of higher expression in cool-acclimated embryos, in particular the red and brown modules. Functional annotation of the red and brown modules revealed distinct biological roles. The red module, composed largely of ribosomal proteins (69 of 75 genes), was enriched for GO terms such as ribonucleoprotein complex subunit organization and regulation of cellular amide metabolic process (**Fig. 5 C**). The brown module, containing 346 genes, was enriched in GO terms including transcription by RNA polymerase III and oxidative phosphorylation (**Fig. 5 C**, **Fig. S10 B**). It is noteworthy that genes in both the red and brown modules were broadly expressed, regardless of cell type, and were more highly expressed in cool-acclimated embryos. The composition of these modules (*i.e.*, predominantly genes related to protein synthesis and energy production) suggests that cool-acclimated embryos were more metabolically active overall than warm-acclimated embryos.

In contrast, the blue, turquoise, black, and yellow modules were expressed more specifically in subsets of certain cell types. The blue module, comprising 371 genes, was primarily expressed in the ectoderm, peripheral nervous system, and ventral nerve cord primordia (**Fig. S9 B**). Enriched GO terms in the blue module included a diverse set of signaling pathways (*e.g.*, Toll, smoothened, and Hippo signaling pathways, and the MAPK cascade) and developmental processes (*e.g.*, axis specification, animal organ formation), reflecting its diverse role for cellular signaling and developmental pathways related to embryonic patterning and tissue development (**Fig. S10 C**). The 559 genes that made up the largest module, turquoise, were the most polarized in their expression across cell types (**Fig. S9 B**). These genes were highly expressed in 5 cell types (ectoderm, peripheral nervous system, ventral nerve cord, foregut & hindgut, tracheal primordia), but were expressed at much lower levels in all other cell types. Similar to the blue module, enriched GO terms from the turquoise module included a diverse array of development and cell signaling pathways (**Fig. S10 E**). The black module (74 genes) was the second smallest module, and was predominantly expressed in the endoderm, ectoderm, and peripheral nervous system primordia (**Fig. S9 B**). There were 11 overrepresented GO terms in the black module, including neuroblast differentiation, peripheral nervous system development, and regulation of cell projection organization, as expected from the cell types that were enriched in this module (**Fig. S10 F**). The yellow module, containing 129 genes, was highly expressed in the amnioserosa, but not in other cell types (**Fig. S9 B**). The yellow module was enriched for GO sets involved in protein processing and cellular organization, response to topologically incorrect protein, response to endoplasmic reticulum stress, Golgi vesicle transport, and protein targeting (**Fig. S10 D**).

Cell-type-specific changes in chromatin accessibility and gene expression across acclimation treatments

Building on the pseudobulk analysis described above, we next examined cell-type-specific changes in chromatin accessibility and gene expression to further explore the molecular basis of thermal acclimation at a finer resolution. In total we identified 161 cell-type specific DARs (**Fig. 6 A**) and 661 cell-type specific DEGs (**Fig. 6 B**). Representative examples of cell-type-specific DEGs were visualized as violin plots (**Fig. S11**). The mesoderm primordium had the most DEGs (296 genes), while the endoderm primordium and amnioserosa were largely unchanged, with only 4 DEGs each. Among the DARs, the ventral nerve cord primordium primarily showed increased accessibility in warm-acclimated embryos compared to cool-acclimated embryos. By contrast, DARs from most other cell types were predominantly more accessible in the cool-acclimated embryos. Interestingly, all 19 DARs in the peripheral nervous system primordia were more accessible in the cool-acclimated embryos, but the 188 DEGs were evenly split between increases and decreases in expression between

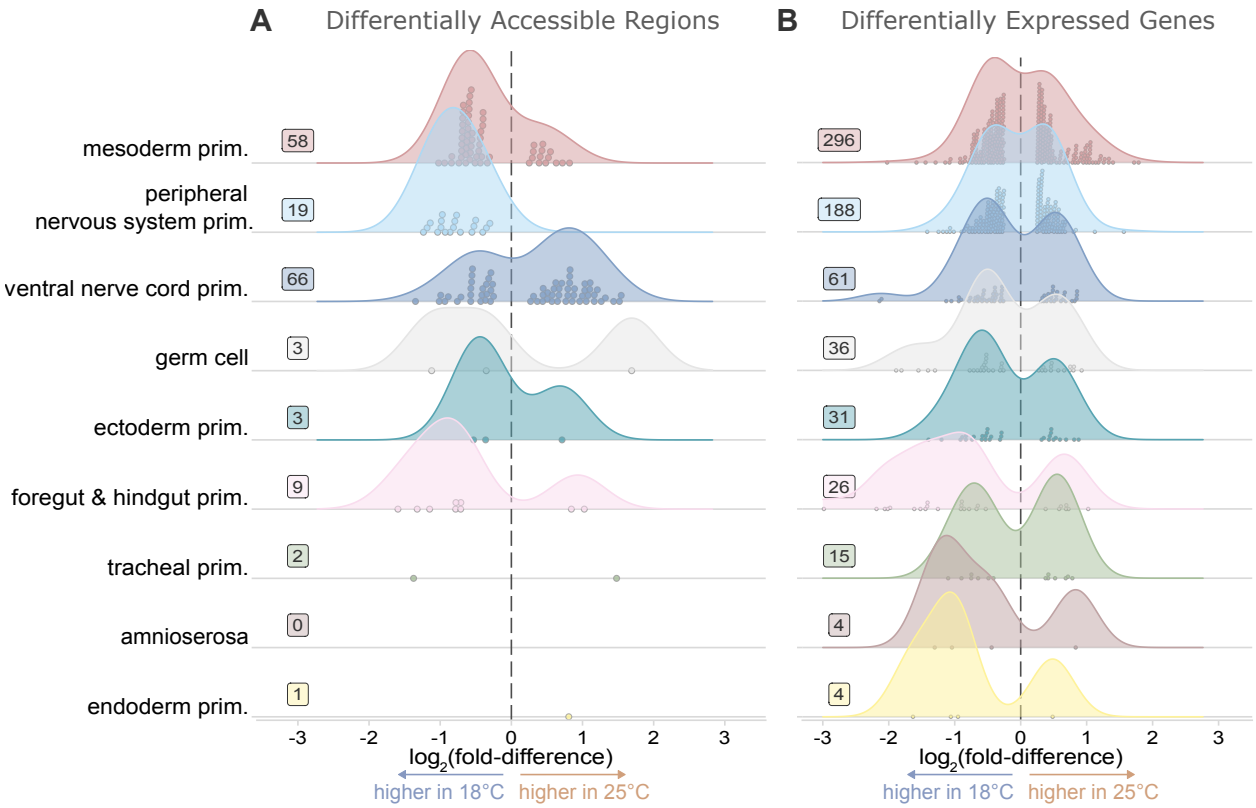

Figure 6: **Gene expression and chromatin accessibility differences following embryonic thermal acclimation.** Density plots of cell-type-specific $\log_2$ fold-differences in accessibility **(A)** and gene expression **(B)**. Only significantly differentially accessible regions (DARs) or differentially expressed genes (DEGs) are plotted (adjusted p-value < 0.05). Primordial cell-types organized from top to bottom by total number of DEGs. Points represent individual regions or genes. Inset number indicates the total number of DARs or DEGs for each cell-type. Color matches cell-type specific UMAP in Fig. 2 C. Positive $\log_2$ fold-difference values indicate expression or accessibility is greater in the 25°C warm-acclimated embryos, and negative values indicate greater expression or accessibility in the 18°C cool-acclimated embryos.

acclimation treatment. The foregut & hindgut primordium showed both increased DARs and DEGs in cool-acclimated embryos, aligning with the signal observed within the Blimp-1 GRN in these tissues (**Fig. 4 B**). In contrast, cell types with the fewest DARs and DEGS, such as trachea, endoderm, and amnioserosa, also lacked any diffGRNs. Notably, the two cell-types with the most DEGs, the mesoderm and peripheral nervous system primordia, correspondingly had the most diffGRNs, with four and three, respectively. Together, these suggest that many of the cell-type-specific changes in accessibility and expression are mediated by the corresponding cell-type-specific GRNs identified by SCENIC+.

Discussion

Here, we demonstrate that *D. melanogaster* embryos exhibited thermal plasticity in upper thermal limits while also maintaining developmental stability in cell type differentiation, chromatin accessibility, and gene expression. Thermal plasticity appears to be underpinned by a homeostatic

response to cool acclimation that we posit comes at the cost of heat tolerance. We did not find evidence that the plasticity in heat tolerance is the result of increased heat-preparedness in warm-acclimated embryos. This conclusion, which we will explore in depth in the following paragraphs, is based on changes in the accessibility of specific target motifs, differences in co-expression modules, and the differential regulation of GRNs.

Embryos displayed a remarkable degree of stability despite temperature variation, maintaining a high degree of similarity in chromatin accessibility and gene expression across cell types. This is evidenced by the extensive overlap in low-dimensional UMAP space of the nuclei from different acclimation treatments, suggesting there was higher variation between cell types than between acclimation treatments. Moreover, less than 2% of tested chromosomal regions and genes showed differential accessibility or expression, highlighting the overall stability of chromatin accessibility and gene expression patterns despite thermal variation. Additionally, more than 97% of the cell-type-specific GRNs we identified had transcription factor expression, target motif accessibility, and/or target gene expression at similar levels between acclimation treatments within a cell type. This observed resilience to environmental variation is in agreement with expectations from previous literature that embryos exhibit remarkably similar patterns of gene expression for certain crucial developmental patterning genes across a wide range of temperatures [12, 13]. However, in response to more extreme temperatures, or in the presence of multiple stressors, thermal acclimation may lead to decreased performance or mortality [50, 46, 51]. In the case of the present study, we exposed embryos to 18°C or 25°C, which is well-within the permissive thermal range of *D. melanogaster* and not likely to induce the potentially detrimental phenotypic consequences of more extreme temperatures [52].

The observation that development at different temperatures yielded identical sets of primordial cell types, yet produced distinct phenotypes—*i.e.*, higher or lower heat tolerance—suggests that the paradigm of environmental robustness of development needs refinement to account for the nuanced molecular responses to environmental variability. The concept of robustness, where there are consistent developmental phenotypic outcomes despite environmental variability, may best describe morphological traits [53, 54, 55]. Whereas other traits, like upper thermal limits, are likely to exhibit a broader range of outcomes, despite the well-established phenomenon of developmental canalization [56, 57]. Both morphological and physiological traits are essential for the survival of the organism and thus have likely undergone intense selection pressures throughout evolutionary history [58, 59, 60]. It may be that selection for morphological canalization favors homeostatic mechanisms that come at the cost of other traits, such as upper thermal limits. We hypothesize that this trade-off arises because the compensatory mechanisms to maintain homeostasis at cooler temperatures, such as increased metabolic activity, create cellular stress during a subsequent heat stress.

Despite the extensive molecular evidence that the developmental program of embryogenesis remains widely conserved across acclimation treatments, we also found evidence of thermal plasticity in both chromatin accessibility and gene expression. Specifically, the concurrent roles of stability and plasticity are most acutely observed at the level of the cell-type-specific GRN, where the vast majority of GRNs were highly resilient to environmental change (*i.e.*, no change in transcription factor expression, target motif accessibility, or target gene expression), and yet there was substantial change in a subset of other GRNs. Among the differential GRNs, six of the eight activator eRegulons showed increased transcription factor expression, increased target motif accessibility, and increased target gene expression in the cool-acclimated embryos relative to the warm-acclimated embryos. This mirrors the signals of increased transcriptional activation and energy production in cool-acclimated embryos observed in the WGCNA analysis, highlighting a potential compensatory mechanism to maintain developmental rates. Specifically in cool-acclimated embryos, we see an

increase in the expression of genes encoding ribosomal proteins, genes involved in transcription, as well as genes related to oxidative phosphorylation. Additionally, in the target motif analysis, we see that cool-acclimated embryos had overall increased accessibility of peaks containing the target motif of Zelda, an early pioneer transcription factor involved in activating the zygotic genome [61, 62, 63].

These patterns are consistent with a homeostatic thermal compensation response to cool acclimation [14, 44, 64], whereby embryos actively increase metabolic activity to overcome slower kinetics at cooler temperatures. This interpretation is supported by a large body of research documenting similar patterns of thermal metabolic compensation across a broad range of taxa [65, 66, 67, 68, 69, 70, 71]. Although, previous work has not described thermal compensation in the context of developmental robustness and typically characterized much longer periods of thermal acclimation. Evidence of complete thermal compensation—*i.e.*, where cold-acclimated organisms exhibit the same biological rates in the cold as warm-acclimated organisms in the heat—has not been documented [14]. Therefore, even though cool-acclimated *D. melanogaster* embryos developed more slowly than warm-acclimated embryos, some level of incomplete thermal compensation may have occurred at a physiological level [72]. It is important to note that the present study was not designed to directly measure biological rate increases, and thus we have no direct evidence of thermal compensation. However, patterns of chromatin accessibility and gene expression in cool- vs. warm-acclimated embryos suggest thermal compensation of biological rates. Follow-up research is required to document the extent to which *D. melanogaster* embryos undergo thermal compensation (*e.g.*, respirometry to measure metabolic rates or nuclear run-on assay to measure active transcription rates).

We propose that these homeostatic responses to cooler temperatures imposed a metabolic burden that reduced heat tolerance. For example, increased rates of protein synthesis would amplify the risk of protein denaturation during heat stress [73, 74]. Similarly, increased rates of oxidative phosphorylation could lead to elevated reactive oxygen species production and oxidative damage [75, 76]. Altogether, these metabolic and cellular stresses would reduce the embryo's ability to cope with acute heat shock—an underappreciated cost of maintaining developmental stability in a variable thermal environment.

In addition to overall signals of thermal compensation, our data further point to a nuanced role of particular cell primordia in mediating thermal responses. The differences in GRNs between acclimation treatments were concentrated in the primordial mesoderm, foregut and hindgut, peripheral nervous system, and ventral nerve cord cell types. To a large degree, this matches the primordial cell types with the most DARs and DEGs, underscoring the role of these cell-type-specific regulators. This also matches the WGCNA results, which showed that genes primarily upregulated in the warm-acclimated embryos were highly expressed in the mesoderm primordium and enriched for GO terms related to muscle development. While some cell-type-specific signatures could arise from variations in developmental timing during embryogenesis, we are confident that our results reflect differences due to acclimation. This is supported by the fact that the hand-staged embryos exhibited overlapping sets of primordial cell types and were undergoing rapid specification at this stage [32], making developmental timing unlikely the sole cause of these observed cell-type-specific signals.

Previous work supports the role of the gut, muscle, and nervous system tissues in thermal stress responses. For example, in adult flies, the maintenance of ion homeostasis in gut and muscle cell membranes is important to cold acclimation and stress tolerance [77, 78, 79, 80]. Also, in adult flies, the heart muscle plays a crucial role in heat tolerance with certain measures of cardiac performance differing in heat-resistant fly lines [81]. In addition, tissue-specific expression of heat shock proteins in the larval gut is protective against cellular damage after acute heat shock [82].

Finally, nervous system function is disrupted at high temperatures as well; however, there is little evidence that it is directly involved in setting the upper thermal limits of adult flies [83]. While some characteristics of primordial embryonic tissues and differentiated larval or adult tissues are similar—*e.g.*, the transcription factors (*e.g.*, *Blimp-1*, *Mef2*, *ab*) that drive the development of the gut, muscle, and nervous system primordia also serve functional roles in differentiated tissue (*e.g.*, ion transport, neuromuscular connections, and contractility) [84, 85, 86]—it is important to note that embryonic tissues differ physiologically from their larval and adult counterparts. Thus, in light of our results, it will be important for future work to investigate the specific roles of the gut, muscle, and nervous system primordia in mediating thermal responses in developing embryos.

Finally, despite the extensive literature to support the hypothesis that higher levels of heat shock protein expression are protective against acute heat shock [74, 40, 41], we did not find any widespread differences in the expression of heat shock genes after acclimation to different temperatures. There is ample evidence of this form of heat preparedness over evolutionary timescales [87, 88, 89] and in the case of heat hardening [90], but heat shock protein expression may play less of a role in the plasticity of upper thermal limits after acclimation within a benign temperature range [91]. Furthermore, it should be noted that chromatin conformation is established prior to heat shock [42], which suggests differences in accessibility of heat shock genes must be established before a heat shock event. However, we found that HSF-motif-containing peaks were more likely to be accessible in the cool-acclimated embryos than in warm-acclimated embryos. In other words, heat shock gene accessibility did not correlate with heat tolerance. Beyond molecular chaperones, there was also little evidence in our results that other protective pathways (*e.g.*, response to oxidative stress) conferred higher heat tolerance in warm-acclimated embryos. We note that a heat-preparedness response may not be triggered in *D. melanogaster* embryos until temperatures higher than 25°C. But considering that warm-acclimated embryos were more heat tolerant than cool-acclimated embryos, we conclude that heat preparedness, at least by the mechanism of heat shock gene expression, was not involved in heat tolerance in the present study.

While the thermal acclimation response of *Drosophila* embryos is consistent with other literature on thermal acclimation across many taxa [92, 93, 94], the speed at which acclimation occurred in *D. melanogaster* embryos is noteworthy. While thermal acclimation is typically reported to occur over days or weeks [95, 96, 97, 98], our findings reveal a rapid acclimation response in *Drosophila* embryos, highlighting potential differences in plasticity between life stages. We note that a beneficial thermal acclimation response—*i.e.*, a positive correlation between acclimation temperature and the associated change in thermal limits—is not always reported in the literature. Many studies show a lack of thermal acclimation at warmer temperatures, and some show a negative correlation between acclimation temperature and upper thermal limits [99, 100, 101]. The lack of a beneficial acclimation response among some taxa may be due to several factors, including behavioral thermoregulation making it unnecessary to evolve a plastic physiological response to temperature [102], as well as the fact that some species and life stages may already live very close to their upper thermal limits and may thus be incapable of extending their upper thermal limit via a plastic response [36, 99]. The observed thermal plasticity in embryos has significant ecological implications, as their immobility and heightened heat sensitivity makes this life stage a critical determinant of survival under fluctuating environmental temperatures [37].

Conclusion

The rapid acclimation in *D. melanogaster* embryos we observed is underpinned by a thermal compensation response, which likely seeks to maintain a robust developmental program of embryogenesis despite variation in temperature. We observe signals of differential regulation at the level of the

cell-type-specific GRN that indicate a homeostatic response to cold-acclimation, which we conclude comes at the cost of increased heat sensitivity due to the metabolic burden, during and after acute heat stress, of increasing transcription, translation, and energy production at lower temperatures. This trade-off between maintaining the pace of development and heat tolerance may be an underappreciated consequence of developmental plasticity, with possible implications for confining plasticity at upper thermal limits. These findings underscore the complexity of thermal acclimation during embryonic development, revealing that plasticity in thermal limits, while adaptive, may be driven in part by the metabolic cost of preserving developmental robustness.

Supporting Information (SI)

See attached Supporting Information (SI) for supplementary figures.

Methods

Fly care

We raised Canton-S flies (Canton, OH, USA) on standard yeast, cornmeal, and molasses food. We maintained stocks at a standard density of approximately 50 to 100 flies per vial (95mm x 25mm, Genesee Scientific) in an incubator (DR-36VL, Percival Scientific Inc.) at 25°C and 55% relative humidity on a 12hr:12hr light:dark cycle. Flies were reared under these conditions for several generations prior to experimentation.

Acclimation and assessing heat tolerance

A few days prior to embryo collections, we transferred approximately 100 mating pairs of 1-2 day-old adult Canton-S flies into small fly cages (Genesee Scientific) with grape juice agar plates (60 x 15 mm) with yeast paste. Fly cages remained in the 25°C incubator. Immediately prior to each experimental collection, we conducted two successive one-hour pre-lays to give the flies fresh egg-laying substrate and reduce the incidence of egg retention. With a fresh agar and yeast plate, we collected embryos for one hour and then transferred the embryos to an incubator at the acclimation treatment temperature (18°C, 25°C, or 30°C). Embryos developed for a certain amount of time based on the expected development rate of their acclimation temperature. We estimated the development times based on a Q_{10} of 2.2 [72]. We subsequently validated these estimated development times by visualizing Browne's stage 11 embryos in each acclimation condition under a light microscope (M80, Leica). Stage 11 embryos were defined as embryos displaying full germ band extension towards the anterior. Control embryos developed at 25°C for 5 hours after egg collection, cool-acclimated embryos developed for 9 hours at 18°C, and the warm-acclimated embryos developed at 30°C for 3 hours.

To assess acute heat tolerance following acclimation, we wrapped egg plates in Parafilm and submerged them in a 38.75°C water bath (A24B, Thermo Scientific) for 45 minutes. Following the heat shock, we placed individual embryos into four-by-five grids of twenty total eggs (Total number of eggs per acclimation temperature: 520, 1272, 1145 for 18°C, 25°C, and 30°C, respectively). The egg plates with gridded embryos recovered from heat shock at 25°C. And finally, we scored hatching success approximately 48 hours after initial egg laying by visualizing hatching under a dissecting microscope. To contrast heat tolerance among acclimation treatments, we conducted a quasi-binomial logistic regression generalized linear model in R on the proportion of eggs hatched after acute heat stress

Embryo acclimation and nuclei extraction for sequencing

Following the heat tolerance results, we chose to move forward with the control (25°C) and cool-acclimated (18°C) embryos for Chromium Single Cell Multiome ATAC + Gene Expression (10X Genomics). We collected and acclimated embryos as above, but immediately following acclimation, we washed and dechorionated the embryos. For each sample, approximately 50 stage 11 embryos were hand-selected and collected with a paintbrush into a 1.5 mL DNA LoBind tube (Eppendorf). We added 100 µL of cryobuffer (90% FBS and 10% DMSO), placed the samples in a isopropanol cryochamber (Cryo-Safe™ Cooler-1°C Freeze Control, Bel-Art Products) and then froze them at -80°C for less than three weeks until nuclei extraction.

Nuclei extraction was completed as described in [103]. In detail, we thawed the cryofrozen embryo samples and subsequently washed the embryos with 250 µL 1x PBS. We centrifuged (Sorvall ST89, Thermo Scientific) the washed samples at 500 RCF for three minutes at 4°C. To the resulting washed embryo pellet, we added 600 µL of lysis buffer (10 mM Tris-HCl, pH 7.5, 10 mM NaCl, 3 mM MgCl 2 , 0.1% IGEPAL, 1% BSA, 1 mM DTT and 1 U/µL RNase Inhibitor – RNaseOUT™ Recombinant Ribonuclease Inhibitor, Thermo Fisher – prepared with nuclease free H2O, and then we transferred the sample to a 1 mL Dounce homogenizer (KIMBLE® KONTES®, Sigma). We homogenized the embryos on ice with the loose pestle for ten passes and then with the tight pestle for an additional ten passes. To decrease loss of sample, we rinsed the pestles with 100 µL of lysis buffer following removal from the sample. We filtered each 800 µL homogenate with a 40 µm Mini-Strainer (pluriSelect) into separate fresh 1.5 mL LoBind tubes. We centrifuged the samples at 900 RCF for five minutes at 4°C. After discarding the supernatant, we washed the the resulting nuclei pellet with 500 µL wash buffer (identical to the Lysis buffer but missing IGEPAL) and centrifuged again at 900 RCF for five minutes at 4°C. Finally, we resuspended the washed nuclei pellet in 20 µL 1X nuclei buffer (10X Genomics) with 1 mM DTT and 1 U/µL RNase Inhibitor.

To assess the quality and concentration of each sample, we visualized an aliquot of isolated nuclei at one-tenth dilution in 1X PBS and 0.1 mg/mL DAPI on a confocal microscope (Nikon ECLIPSE Ti2). We confirmed nuclei quality by looking for the absence of nuclear blebbing at 600X magnification. All visualized nuclei were high-quality or mostly intact with minor evidence of blebbing as defined by 10X Genomics. We estimated nuclei concentration by loading 10 µL of one-tenth diluted sample onto a hemocytometer (Bright-Line™, American Optical) and visualized nuclei with DAPI fluorescence on the confocal microscope at 100X magnification.

Prior to proceeding to 10X Genomics Chromium Single Cell Multiome ATAC + Gene Expression sequencing library preparation, we diluted each sample to an estimated concentration of 2,000 nuclei per µL with 1X nuclei buffer.

Library preparation and sequencing

Vermont Integrative Genomics Resource (VIGR) conducted the ATAC and GEX library preparation following the 10X Genomics protocol (Chromium Next GEM Multiome ATAC + Gene Expression User Guide, Document Number CG000338, Rev F, August 2022). We targeted 4,000 total nuclei per sample. Briefly, each sample of nuclei was transposed and then loaded onto a Chromium Next GEM Chip J to generate GEMs and barcode individual nuclei. After the GEMs are broken down, barcoded transposed DNA and cDNA are amplified with PCR. And finally, the individual ATAC and Gene Expression libraries were constructed and then sequenced on a rapid-run flow cell on an Ilumina Hi-Seq 2500™.

Sequencing analysis

We conducted all sequence processing on the Vermont Advanced Computing Core (VACC). Sequencing reads were demultiplexed and analyzed with the Cell Ranger ARC, version 2.0.2 (10X Genomics) pipeline as recommended. In detail, a *D. melanogaster* reference package was created following 10X Genomics recommendations. The FASTA (BDGP6.32) and GTF (BDGP6.32.109) files were downloaded from Ensembl database. Prior to creating the reference package, the GTF file was filtered so that the reference was restricted to protein coding, long non-coding RNA, antisense, and immune-related genes, the same filter criteria used by 10X Genomics to create the human and mouse references.

Then, the Cell Ranger ARC pipeline was run on all samples to trim, align, and map reads, and then create count matrices for gene expression and chromatin accessibility peaks. Samples were then aggregated together into a single file for each data type and then the files were imported into R version 4.2.2 [104] and analyzed using Seurat version 4.4.0 [105] and Signac 1.12.0 [106]. Subsequently, we used python version 3.8.18 to model cis-regulatory topics using pycisTopic version 1.0.3 [107], then transcription factor motif enrichment using pycisTarget version 1.0.3, and finally identified enhancer-driven gene regulatory networks using SCENIC+ version 1.0.1 [49]. All code used for the analysis is available on GitHub at https://github.com/tsoleary/heater.

Quality control filtering

In detail, single GEM barcodes were filtered to high quality nuclei based on several criteria: i. a low-count threshold for both the ATAC and RNA libraries (≥ 800 and ≥ 200 counts per barcode respectively), ii. a maximum cut-off for percentage of reads mapped to mitochondrial transcripts ($< 5\%$) and ribosomal genes ($< 25\%$), iii. putative multiplets were identified using AMULET for the ATAC-seq libraries [108] and DoubletFinder for the RNA-seq libraries [109]. Finally, all barcodes clustering with a high number of putative multiples, defined as clusters with greater than 15% multiplets, were removed. This filtering left 10,390 high-quality nuclei for all downstream analysis. Due to the high cell-cycle heterogeneity expected in developmental tissue, genes known to change across cell cycle phases, were regressed out of the snRNA data [105]. We called chromatin accessibility peaks using macs2 version 2.2.7.1 [110]. And finally, the RNA and ATAC data were analyzed by Seurat according to current recommendations [106, 111].

Clustering and annotating cell-types

We identified clusters using the joint ATAC and RNA data with use of the FindMultiModalNeighbors and FindClusters function in Seurat. We tested multiple clustering resolutions ranging from 0.1 to 1, and settled on a resolution of 0.7 (**Fig. S3**). We then used the gene expression information to identify marker genes for each cluster using the FindConservedMarkers function. The clusters were assigned annotated cell-types by conducting a test of Fisher's enrichment on marker genes annotated by the Berkley *Drosophila* Genome Project RNA in situ hybridization database [4, 29, 2].

Differentially enriched motifs in pseudobulk DARs

We tested for differentially enriched motifs using the FindMotifs function in Seurat. *D. melanogaster* motifs were identified using the transcription factor binding profiles from JASPAR 2022 [112].

Cell-type-specific differential expression and accessibility testing

Using Seurat, we ran differential accessibility and expression testing between acclimation treatments but within cell types using MAST [113] with the FindMarkers function in Seurat. In addition to a Bonferroni adjusted p-value less than 0.05, differentially accessibility regions (DARs) or differentially expressed genes (DEGs) needed to be present in greater than 10% of nuclei tested and a have minimum absolute-value of $\log_2$ fold-difference of 0.25.

Weighted gene co-expression network analysis (hdWGCNA)

We conducted a high dimensional weighted gene co-expression network analysis with hdWGCNA [114];, version 0.2.27, on the single-nuclei RNA data to identify modules of genes that are expressed in similar patterns as well as modules that are different between acclimation conditions. Differential module eigengenes between acclimation conditions were identified using the FindDMEs function using MAST similar to the individual DEG and DAR testing as described above.

Identifying enhancer driven gene regulatory networks using SCENIC+

SCENIC+ (version 1.0.1) was used to identify gene regulatory networks (GRNs). Using the single-nuclei ATAC-seq data, cis-regulatory topics were modeled using cisTopic [107], and cisTarget was then used for motif enrichment and identifying transcription factor cistromes. SCENIC+ was used to identify cell-type-specific enhancer driven gene regulatory networks (GRNs) by using the linked gene expression data from the single-nuclei RNA-seq [49]. We tested for differential GRNs (diffGRNs) that were altered by acclimation using a three-part test: i. the transcription factor is differentially expressed within the cell-type (DEGs MAST; $|\text{lfc}| > 0.25$, adjusted p-value < 0.05, percent nuclei expressed $> 10\%$), ii. the distribution of $\log_2$ fold-differences of the regions containing the target motif are shifted non-zero in the direction expected by its activator or repressor label (one-sample t-test; $p < 0.05$), and finally, iii. the distribution of $\log_2$ fold-differences of the corresponding target genes are altered in the same way (one-sample t-test; $p < 0.05$). This method tests for GRNs that have changed their transcription factor expression, target motif accessibility, and target gene expression as a result of acclimation.

Acknowledgements

We thank Kristi Montooth, Colin Meiklejohn, and Princess Rodriguez for helpful discussions. This work was supported by NSF grant OIA-1826689 to SHC, SF, and BLL. VIGR is supported by grant U54 GM115516 from the National Institutes of Health for the Northern New England Clinical and Translational Research Network.

References

[1] Thomas Gregor et al. "Probing the limits to positional information". en. In: *Cell* 130.1 (July 2007), pp. 153–164.

[2] Ann S Hammonds et al. "Spatial expression of transcription factors in Drosophila embryonic organ development". en. In: *Genome Biol.* 14.12 (Dec. 2013), R140.

[3] Melissa M Harrison, Audrey J Marsh, and Christine A Rushlow. "Setting the stage for development: the maternal-to-zygotic transition in Drosophila". en. In: *Genetics* 225.2 (Oct. 2023).

[4] Pavel Tomancak et al. “Global analysis of patterns of gene expression during Drosophila embryogenesis”. en. In: *Genome Biol.* 8.7 (2007), R145.

[5] Elham Gheisari, Mostafa Aakhte, and H-Arno J Müller. “Gastrulation in Drosophila melanogaster: Genetic control, cellular basis and biomechanics”. en. In: *Mech. Dev.* 163 (Sept. 2020), p. 103629.

[6] Shigeo Hayashi and Takefumi Kondo. “Development and Function of the Drosophila Tracheal System”. en. In: *Genetics* 209.2 (June 2018), pp. 367–380.

[7] Adam C Martin. “The Physical Mechanisms of Drosophila Gastrulation: Mesoderm and Endoderm Invagination”. en. In: *Genetics* 214.3 (Mar. 2020), pp. 543–560.

[8] Jingjing Sun et al. “Collective Migrations of Drosophila Embryonic Trunk and Caudal Mesoderm-Derived Muscle Precursor Cells”. en. In: *Genetics* 215.2 (June 2020), pp. 297–322.

[9] Monika Hilker, Hassan Salem, and Nina E Fatouros. “Adaptive Plasticity of Insect Eggs in Response to Environmental Challenges”. en. In: *Annu. Rev. Entomol.* (Oct. 2022).

[10] Christen K Mirth, Timothy E Saunders, and Christopher Amourda. “Growing Up in a Changing World: Environmental Regulation of Development in Insects”. en. In: *Annu. Rev. Entomol.* 66 (Jan. 2021), pp. 81–99.

[11] David Cheung and Jun Ma. “Probing the impact of temperature on molecular events in a developmental system”. en. In: *Sci. Rep.* 5 (Aug. 2015), p. 13124.

[12] Avigdor Eldar et al. “Robustness of the BMP morphogen gradient in Drosophila embryonic patterning”. en. In: *Nature* 419.6904 (Sept. 2002), pp. 304–308.

[13] Elena M Lucchetta et al. “Dynamics of Drosophila embryonic patterning network perturbed in space and time using microfluidics”. en. In: *Nature* 434.7037 (Apr. 2005), pp. 1134–1138.

[14] George N Somero, Brent L Lockwood, and Lars Tomanek. *Biochemical Adaptation: Response to Environmental Challenges, from Life’s Origins to the Anthropocene*. Sunderland, MA: Sinauer Associates, Inc, 2017.

[15] Marta Benet et al. “Modulation of protein synthesis and degradation maintains proteostasis during yeast growth at different temperatures”. en. In: *Biochim. Biophys. Acta Gene Regul. Mech.* 1860.7 (July 2017), pp. 794–802.

[16] José E Pérez-Ortín, Paula M Alepuz, and Joaquín Moreno. “Genomics and gene transcription kinetics in yeast”. en. In: *Trends Genet.* 23.5 (May 2007), pp. 250–257.

[17] D J Coughlin et al. “Thermal acclimation and gene expression in rainbow smelt: Changes in the myotomal transcriptome in the cold”. en. In: *Comp. Biochem. Physiol. Part D Genomics Proteomics* 31 (Sept. 2019), p. 100610.

[18] Heath A MacMillan et al. “Cold acclimation wholly reorganizes the Drosophila melanogaster transcriptome and metabolome”. en. In: *Sci. Rep.* 6 (June 2016), p. 28999.

[19] Torsten N Kristensen et al. “Proteomic data reveal a physiological basis for costs and benefits associated with thermal acclimation”. en. In: *J. Exp. Biol.* 219.Pt 7 (Apr. 2016), pp. 969–976.

[20] Tetsuhiro S Hatakeyama and Kunihiko Kaneko. “A linear reciprocal relationship between robustness and plasticity in homeostatic biological networks”. en. In: *PLoS One* 18.1 (Jan. 2023), e0277181.

[21] H Frederik Nijhout, Janet A Best, and Michael C Reed. "Systems biology of robustness and homeostatic mechanisms". en. In: *Wiley Interdiscip. Rev. Syst. Biol. Med.* 11.3 (May 2019), e1440.

[22] H Frederik Nijhout and Michael C Reed. "Homeostasis and dynamic stability of the phenotype link robustness and plasticity". en. In: *Integr. Comp. Biol.* 54.2 (July 2014), pp. 264–275.

[23] G N Somero. "The physiology of climate change: how potentials for acclimatization and genetic adaptation will determine 'winners' and 'losers'". en. In: *J. Exp. Biol.* 213.6 (Mar. 2010), pp. 912–920.

[24] Carla M Sgrò, John S Terblanche, and Ary A Hoffmann. "What Can Plasticity Contribute to Insect Responses to Climate Change?" In: *Annu. Rev. Entomol.* 61.1 (Mar. 2016), pp. 433–451.

[25] David Berrigan. "Acclimation of metabolic rate in response to developmental temperature in Drosophila melanogaster". In: *J. Therm. Biol.* 22.3 (June 1997), pp. 213–218.

[26] Wael Tadros and Howard D Lipshitz. "The maternal-to-zygotic transition: a play in two acts". en. In: *Development* 136.18 (Sept. 2009), pp. 3033–3042.

[27] Nadine L Vastenhouw, Wen Xi Cao, and Howard D Lipshitz. "The maternal-to-zygotic transition revisited". en. In: *Development* 146.11 (June 2019).

[28] D Loncar and S J Singer. "Cell membrane formation during the cellularization of the syncytial blastoderm of Drosophila". en. In: *Proc. Natl. Acad. Sci. U. S. A.* 92.6 (Mar. 1995), pp. 2199–2203.

[29] Pavel Tomancak et al. "Systematic determination of patterns of gene expression during Drosophila embryogenesis". en. In: *Genome Biol.* 3.12 (Dec. 2002), RESEARCH0088.

[30] Tim Pollex et al. "Enhancer-promoter interactions become more instructive in the transition from cell-fate specification to tissue differentiation". en. In: *Nat. Genet.* (Mar. 2024).

[31] Danielle C Hamm and Melissa M Harrison. "Regulatory principles governing the maternal-to-zygotic transition: insights from Drosophila melanogaster". en. In: *Open Biol.* 8.12 (Dec. 2018), p. 180183.

[32] Diego Calderon et al. "The continuum of Drosophila embryonic development at single-cell resolution". en. In: *Science* 377.6606 (Aug. 2022), eabn5800.

[33] Jennifer M Sunday, Amanda E Bates, and Nicholas K Dulvy. "Global analysis of thermal tolerance and latitude in ectotherms". en. In: *Proc. Biol. Sci.* 278.1713 (June 2011), pp. 1823–1830.

[34] Brent J Sinclair et al. "Can we predict ectotherm responses to climate change using thermal performance curves and body temperatures?" en. In: *Ecol. Lett.* 19.11 (Nov. 2016), pp. 1372–1385.

[35] A A Hoffmann. "Physiological climatic limits in Drosophila: patterns and implications". en. In: *J. Exp. Biol.* 213.6 (Mar. 2010), pp. 870–880.

[36] Jonathon H Stillman. "Acclimation capacity underlies susceptibility to climate change". en. In: *Science* 301.5629 (July 2003), p. 65.

[37] Brent L Lockwood, T Gupta, and R Scavotto. "Disparate patterns of thermal adaptation between life stages in temperate vs. tropical Drosophila melanogaster". en. In: *J. Evol. Biol.* 31.2 (Feb. 2018), pp. 323–331.

[38] Jennifer M Sunday et al. “Thermal-safety margins and the necessity of thermoregulatory behavior across latitude and elevation”. en. In: *Proc. Natl. Acad. Sci. U. S. A.* 111.15 (Apr. 2014), pp. 5610–5615.

[39] Robbie S Wilson and Craig E Franklin. “Testing the beneficial acclimation hypothesis”. en. In: *Trends Ecol. Evol.* 17.2 (Feb. 2002), pp. 66–70.

[40] Brent L Lockwood, Cole R Julick, and Kristi L Montooth. “Maternal loading of a small heat shock protein increases embryo thermal tolerance in Drosophila melanogaster”. en. In: *J. Exp. Biol.* 220.Pt 23 (Dec. 2017), pp. 4492–4501.

[41] Lori A Manzon et al. “Thermal acclimation alters both basal heat shock protein gene expression and the heat shock response in juvenile lake whitefish (Coregonus clupeaformis)”. en. In: *J. Therm. Biol.* 104 (Feb. 2022), p. 103185.

[42] Judhajeet Ray et al. “Chromatin conformation remains stable upon extensive transcriptional changes driven by heat shock”. en. In: *Proc. Natl. Acad. Sci. U. S. A.* 116.39 (Sept. 2019), pp. 19431–19439.

[43] Xiaona Shen et al. “Characteristics of the Accessible Chromatin Landscape and Transcriptome under Different Temperature Stresses in Bemisia tabaci”. en. In: *Genes* 14.10 (Oct. 2023).

[44] Theodore Holmes Bullock. “COMPENSATION FOR TEMPERATURE IN THE METABOLISM AND ACTIVITY OF POIKILOTHERMS”. en. In: *Biological Reviews* 30.3 (Aug. 1955), pp. 311–342.

[45] Matti Vornanen et al. “Steady-state effects of temperature acclimation on the transcriptome of the rainbow trout heart”. en. In: *Am. J. Physiol. Regul. Integr. Comp. Physiol.* 289.4 (Oct. 2005), R1177–84.

[46] Peter Klepsatel et al. “Thermal stress depletes energy reserves in Drosophila”. en. In: *Sci. Rep.* 6 (Sept. 2016), p. 33667.

[47] Peter Klepsatel, David Wildridge, and Martina Gáliková. “Temperature induces changes in Drosophila energy stores”. en. In: *Sci. Rep.* 9.1 (Mar. 2019), p. 5239.

[48] Erwin Frise, Ann S Hammonds, and Susan E Celniker. “Systematic image-driven analysis of the spatial Drosophila embryonic expression landscape”. en. In: *Mol. Syst. Biol.* 6 (Jan. 2010), p. 345.

[49] Carmen Bravo González-Blas et al. “SCENIC+: single-cell multiomic inference of enhancers and gene regulatory networks”. en. In: *Nat. Methods* (July 2023).

[50] Volker Loeschcke and Ary A Hoffmann. “Consequences of heat hardening on a field fitness component in Drosophila depend on environmental temperature”. en. In: *Am. Nat.* 169.2 (Feb. 2007), pp. 175–183.

[51] J-L Da Lage, P Capy, and J-R David. “Starvation and desiccation tolerance in Drosophila melanogaster adults: Effects of environmental temperature”. en. In: *J. Insect Physiol.* 35.6 (Jan. 1989), pp. 453–457.

[52] Mads F Schou et al. “Metabolic and functional characterization of effects of developmental temperature in Drosophila melanogaster”. en. In: *Am. J. Physiol. Regul. Integr. Comp. Physiol.* 312.2 (Feb. 2017), R211–R222.

[53] C H Waddington. “CANALIZATION OF DEVELOPMENT AND THE INHERITANCE OF ACQUIRED CHARACTERS”. en. In: *Nature* 150.3811 (Nov. 1942), pp. 563–565.

[54] Mark L Siegal and Aviv Bergman. "Waddington's canalization revisited: developmental stability and evolution". en. In: *Proc. Natl. Acad. Sci. U. S. A.* 99.16 (Aug. 2002), pp. 10528–10532.

[55] Thomas Flatt. "The evolutionary genetics of canalization". en. In: *Q. Rev. Biol.* 80.3 (Sept. 2005), pp. 287–316.

[56] C K Ghalambor et al. "Adaptive versus non-adaptive phenotypic plasticity and the potential for contemporary adaptation in new environments". en. In: *Funct. Ecol.* 21.3 (June 2007), pp. 394–407.

[57] C M Sgrò and A A Hoffmann. "Genetic correlations, tradeoffs and environmental variation". en. In: *Heredity (Edinb.)* 93.3 (Sept. 2004), pp. 241–248.

[58] S Elena and R Lenski. "Microbial genetics: Evolution experiments with microorganisms: the dynamics and genetic bases of adaptation". In: *Nat. Rev. Genet.* 4.6 (2003), pp. 457–469.

[59] Michael J Angilletta Jr, Todd D Steury, and Michael W Sears. "Temperature, growth rate, and body size in ectotherms: fitting pieces of a life-history puzzle". en. In: *Integr. Comp. Biol.* 44.6 (Dec. 2004), pp. 498–509.

[60] Molly K Burke et al. "Genome-wide analysis of a long-term evolution experiment with Drosophila". en. In: *Nature* 467.7315 (Sept. 2010), pp. 587–590.

[61] Melissa M Harrison et al. "Zelda binding in the early Drosophila melanogaster embryo marks regions subsequently activated at the maternal-to-zygotic transition". en. In: *PLoS Genet.* 7.10 (Oct. 2011), e1002266.

[62] Katharine N Schulz et al. "Zelda is differentially required for chromatin accessibility, transcription factor binding, and gene expression in the early Drosophila embryo". en. In: *Genome Res.* 25.11 (Nov. 2015), pp. 1715–1726.

[63] Xiao-Yong Li et al. "Establishment of regions of genomic activity during the Drosophila maternal to zygotic transition". In: *Elife* 3 (Oct. 2014), e03737.

[64] F E Fry. "Temperature compensation". en. In: *Annu. Rev. Physiol.* 20.1 (Mar. 1958), pp. 207–224.

[65] J R Hazel and C L Prosser. "Molecular mechanisms of temperature compensation in poikilotherms". en. In: *Physiol. Rev.* 54.3 (July 1974), pp. 620–677.

[66] Pénélope Tarapacki et al. "Acclimation, duration and intensity of cold exposure determine the rate of cold stress accumulation and mortality in Drosophila suzukii". en. In: *J. Insect Physiol.* 135 (Oct. 2021), p. 104323.

[67] B L Coggins et al. "Breaking free from thermodynamic constraints: thermal acclimation and metabolic compensation in a freshwater zooplankton species". en. In: *J. Exp. Biol.* 224.Pt 4 (Feb. 2021).

[68] Madison L Earhart et al. "Heatwave resilience of juvenile white sturgeon is associated with epigenetic and transcriptional alterations". en. In: *Sci. Rep.* 13.1 (Sept. 2023), p. 15451.

[69] A M Burnell, C Reaper, and J Doherty. "The effect of acclimation temperature on enzyme activity in Drosophila melanogaster". en. In: *Comp. Biochem. Physiol. B* 98.4 (1991), pp. 609–614.

[70] Brent L Lockwood and George N Somero. "Invasive and native blue mussels (genus Mytilus) on the California coast: The role of physiology in a biological invasion". In: *J. Exp. Mar. Bio. Ecol.* 400.1 (Apr. 2011), pp. 167–174.

[71] Nicolas Pichaud et al. “Adjustments of cardiac mitochondrial phenotype in a warmer thermal habitat is associated with oxidative stress in European perch, Perca fluviatilis”. en. In: *Sci. Rep.* 10.1 (Oct. 2020), p. 17697.

[72] Steven G Kuntz and Michael B Eisen. “Drosophila embryogenesis scales uniformly across temperature in developmentally diverse species”. en. In: *PLoS Genet.* 10.4 (Apr. 2014), e1004293.

[73] M E Feder and G E Hofmann. “Heat-shock proteins, molecular chaperones, and the stress response: evolutionary and ecological physiology”. en. In: *Annu. Rev. Physiol.* 61 (1999), pp. 243–282.

[74] J G Sørensen, T N Kristensen, and V Loeschcke. “The evolutionary and ecological role of heat shock proteins”. In: *Ecol. Lett.* (2003).

[75] Imen Belhadj Slimen et al. “Reactive oxygen species, heat stress and oxidative-induced mitochondrial damage. A review”. In: *Int. J. Hyperthermia* 30.7 (Nov. 2014), pp. 513–523.

[76] Xingzhi Han et al. “Metabolic regulation reduces the oxidative damage of arid lizards in response to moderate heat events”. en. In: *Integr. Zool.* (Oct. 2023).

[77] Alexandra Cheslock, Mads Kuhlmann Andersen, and Heath A MacMillan. “Thermal acclimation alters Na+/K+-ATPase activity in a tissue-specific manner in Drosophila melanogaster”. en. In: *Comp. Biochem. Physiol. A Mol. Integr. Physiol.* 256 (June 2021), p. 110934.

[78] Jeppe Seamus Bayley et al. “Cold acclimation increases depolarization resistance and tolerance in muscle fibers from a chill-susceptible insect, *Locusta migratoria*”. In: *American Journal of Physiology-Regulatory, Integrative and Comparative Physiology* 319.4 (Oct. 2020), R439–R447.

[79] Heath A MacMillan et al. “Thermal acclimation mitigates cold-induced paracellular leak from the Drosophila gut”. en. In: *Sci. Rep.* 7.1 (Aug. 2017), p. 8807.

[80] Gil Y Yerushalmi et al. “Functional plasticity of the gut and the Malpighian tubules underlies cold acclimation and mitigates cold-induced hyperkalemia in Drosophila melanogaster”. en. In: *J. Exp. Biol.* 221.Pt 6 (Mar. 2018), jeb174904.

[81] Maia Rodríguez et al. “Cardiac performance in heat-stressed flies of heat-susceptible and heat-resistant Drosophila melanogaster”. en. In: *J. Insect Physiol.* 133 (Aug. 2021), p. 104268.

[82] R A Krebs and M E Feder. “Tissue-specific variation in Hsp70 expression and thermal damage in Drosophila melanogaster larvae”. en. In: *J. Exp. Biol.* 200.Pt 14 (July 1997), pp. 2007–2015.

[83] Lisa B Jørgensen, R Meldrum Robertson, and Johannes Overgaard. “Neural dysfunction correlates with heat coma and CTmax in Drosophila but does not set the boundaries for heat stress survival”. en. In: *J. Exp. Biol.* 223.Pt 13 (July 2020).

[84] Anton L Bryantsev et al. “Differential requirements for Myocyte Enhancer Factor-2 during adult myogenesis in Drosophila”. en. In: *Dev. Biol.* 361.2 (Jan. 2012), pp. 191–207.

[85] Florence J Blanchard et al. “The transcription factor Mef2 is required for normal circadian behavior in Drosophila”. en. In: *J. Neurosci.* 30.17 (Apr. 2010), pp. 5855–5865.

[86] Moustafa Sarhan, Koichi Miyagawa, and Hitoshi Ueda. “Domain analysis of Drosophila Blimp-1 reveals the importance of its repression function and instability in determining pupation timing”. en. In: *Genes Cells* 28.5 (May 2023), pp. 338–347.

[87] Yunwei Dong et al. “Heat-shock protein 70 (Hsp70) expression in four limpets of the genus Lottia: interspecific variation in constitutive and inducible synthesis correlates with in situ exposure to heat stress”. en. In: *Biol. Bull.* 215.2 (Oct. 2008), pp. 173–181.

[88] Emily E Mikucki, Thomas S O’Leary, and Brent L Lockwood. “Heat tolerance, oxidative stress response tuning, and robust gene activation in early-stage Drosophila melanogaster embryos”. en. In: *bioRxiv* (Apr. 2024), p. 2024.04.29.591747.

[89] Bing Chen, Martin E Feder, and Le Kang. “Evolution of heat-shock protein expression underlying adaptive responses to environmental stress”. en. In: *Mol. Ecol.* 27.15 (Aug. 2018), pp. 3040–3054.

[90] Jesper Givskov Sørensen et al. “Expression of thermal tolerance genes in two Drosophila species with different acclimation capacities”. en. In: *J. Therm. Biol.* 84 (Aug. 2019), pp. 200–207.

[91] Nishad Jayasundara et al. “Proteomic analysis of cardiac response to thermal acclimation in the eurythermal goby fish Gillichthys mirabilis”. en. In: *J. Exp. Biol.* 218.Pt 9 (May 2015), pp. 1359–1372.

[92] Rachael Morgan et al. “Are model organisms representative for climate change research? Testing thermal tolerance in wild and laboratory zebrafish populations”. en. In: *Conserv. Physiol.* 7.1 (June 2019), coz036.

[93] Lise Comte and Julian D Olden. “Evolutionary and environmental determinants of freshwater fish thermal tolerance and plasticity”. en. In: *Glob. Chang. Biol.* 23.2 (Feb. 2017), pp. 728–736.

[94] Thomas Enriquez and Hervé Colinet. “Cold acclimation triggers major transcriptional changes in Drosophila suzukii”. en. In: *BMC Genomics* 20.1 (May 2019), p. 413.

[95] A R Cossins. “Adaptation of biological membranes to temperature. The effect of temperature acclimation of goldfish upon the viscosity of synaptosomal membranes”. en. In: *Biochim. Biophys. Acta* 470.3 (Nov. 1977), pp. 395–411.

[96] Michael J Angilletta Jr, Catriona Condon, and Jacob P Youngblood. “Thermal acclimation of flies from three populations of Drosophila melanogaster fails to support the seasonality hypothesis”. en. In: *J. Therm. Biol.* 81 (Apr. 2019), pp. 25–32.

[97] Johannes Overgaard et al. “Effects of acclimation temperature on thermal tolerance and membrane phospholipid composition in the fruit fly Drosophila melanogaster”. en. In: *J. Insect Physiol.* 54.3 (Mar. 2008), pp. 619–629.

[98] Thomas Enriquez and Hervé Colinet. “Cold acclimation triggers lipidomic and metabolic adjustments in the spotted wing drosophila Drosophila suzukii (Matsumara)”. en. In: *Am. J. Physiol. Regul. Integr. Comp. Physiol.* 316.6 (June 2019), R751–R763.

[99] Belinda Heerwaarden, Vanessa Kellermann, and Carla M Sgrò. “Limited scope for plasticity to increase upper thermal limits”. en. In: *Funct. Ecol.* 30.12 (Dec. 2016), pp. 1947–1956.

[100] Mads Fristrup Schou et al. “Linear reaction norms of thermal limits in Drosophila : predictable plasticity in cold but not in heat tolerance”. en. In: *Funct. Ecol.* 31.4 (Apr. 2017), pp. 934–945.

[101] Seema Ramniwas, Girish Kumar, and Divya Singh. “Rejection of the beneficial acclimation hypothesis (BAH) for short term heat acclimation in Drosophila nepalensis”. en. In: *Genetica* 148.3-4 (Aug. 2020), pp. 173–182.

[102] Elrike Marais and Steven L Chown. "Beneficial acclimation and the Bogert effect". en. In: *Ecol. Lett.* 11.10 (Oct. 2008), pp. 1027–1036.

[103] Ashley R Albright, Michael R Stadler, and Michael B Eisen. "Single-nucleus RNA-sequencing in pre-cellularization Drosophila melanogaster embryos". en. In: *PLoS One* 17.6 (June 2022), e0270471.

[104] R Core Team. *R: A Language and Environment for Statistical Computing.* Vienna, Austria, 2020.

[105] Andrew Butler et al. "Integrating single-cell transcriptomic data across different conditions, technologies, and species". en. In: *Nat. Biotechnol.* 36.5 (June 2018), pp. 411–420.

[106] Tim Stuart et al. "Single-cell chromatin state analysis with Signac". en. In: *Nat. Methods* 18.11 (Nov. 2021), pp. 1333–1341.

[107] Carmen Bravo González-Blas et al. "cisTopic: cis-regulatory topic modeling on single-cell ATAC-seq data". en. In: *Nat. Methods* 16.5 (May 2019), pp. 397–400.

[108] Asa Thibodeau et al. "AMULET: a novel read count-based method for effective multiplet detection from single nucleus ATAC-seq data". en. In: *Genome Biol.* 22.1 (Sept. 2021), p. 252.

[109] Christopher S McGinnis, Lyndsay M Murrow, and Zev J Gartner. "DoubletFinder: Doublet Detection in Single-Cell RNA Sequencing Data Using Artificial Nearest Neighbors". en. In: *Cell Syst* 8.4 (Apr. 2019), 329–337.e4.

[110] Yong Zhang et al. "Model-based analysis of ChIP-Seq (MACS)". en. In: *Genome Biol.* 9.9 (Sept. 2008), R137.

[111] Christoph Hafemeister and Rahul Satija. "Normalization and variance stabilization of single-cell RNA-seq data using regularized negative binomial regression". en. In: *Genome Biol.* 20.1 (Dec. 2019), p. 296.

[112] Jaime A Castro-Mondragon et al. "JASPAR 2022: the 9th release of the open-access database of transcription factor binding profiles". en. In: *Nucleic Acids Res.* 50.D1 (Jan. 2022), pp. D165–D173.

[113] Greg Finak et al. "MAST: a flexible statistical framework for assessing transcriptional changes and characterizing heterogeneity in single-cell RNA sequencing data". en. In: *Genome Biol.* 16 (Dec. 2015), p. 278.

[114] Samuel Morabito et al. "hdWGCNA identifies co-expression networks in high-dimensional transcriptomics data". en. In: *Cell Rep Methods* 3.6 (June 2023), p. 100498.